Master's Thesis

Isolation of Cytochrome P450 74 Family Gene from *Vitis vinifera* L. and Characterization of Its Recombinant Protein

Jinkyu Woo

Department of Biotechnology
GRADUATE SCHOOL
JEJU NATIONAL UNIVERSITY

December, 2011

Master's Thesis

Isolation of Cytochrome P450 74 Family Gene from *Vitis vinifera* L. and Characterization of Its Recombinant Protein

Jinkyu Woo

Department of Biotechnology
GRADUATE SCHOOL
JEJU NATIONAL UNIVERSITY

December, 2011

Isolation of Cytochrome P450 74 Family Gene from *Vitis vinifera* L. and Characterization of Its Recombinant Protein

Jinkyu Woo

(Supervised by professor Key-Zung Riu and Dong-Sun Lee)

A thesis submitted in partial fulfillment of the requirement
for the degree of Master of Biotechnology

December, 2011

This thesis has been examined and approved by

_____

Chairperson of the supervising committees

Pyung-Ok Lim, Ph.D., Department of Science Education, Jeju National University

_____

Key-Zung Riu, Ph.D., College of Applied Life Sciences, Jeju National University

_____

Dong-Sun Lee, Ph.D., College of Applied Life Sciences, Jeju National University

Department of Biotechnology
GRADUATE SCHOOL
JEJU NATIONAL UNIVERSITY

CONTENTS

ABBREVIATIONS

CYP	Cytochrome P450
PCR	Polymerase chain reaction
Ni^{2+}-NTA	Nickel- nitrilotriacetic acid
SDS-PAGE	Sodium dodecyl sulfate- polyacrylamide gel electrophoresis
GC/MS	Gas-liquid Chromatography/mass spectrometry
UV/VIS	Ultraviolet/visible
δ-ALA	5-Aminolevulinic acid hydrochloride
LOX	Lipoxygenase
AOS	Allene oxide synthase
HPL	Hydroperoxide lyase
DES	Divinyl ether synthase
EAS	Epoxy alcohol synthase
9-HPOD	(9S,10E,12Z,15Z)-9-Hydroperoxy-10,12,15-octadecatrieoic acid
13-HPOD	(9S,11E,13S,15Z)-13-Hydroperoxy-9,11,15-octadecatrieoic acid
O. G.	n-Octyl-β-D-Glucopyranoside
VvCYP74	Cytochrome p450 74 family gene isolated from *Vitis vinifera* L.

LIST OF FIGURES

LIST OF TABLES

SUMMARY

In order to identify gene function related to oxylipin biosynthesis, cytochrome P450 (CYP450) 74 family gene was isolated from grape, *Vitis vinifera* L. The length of this gene was 1,452 bp in nucleotide sequences, which encoded 479 amino acids. Through bioinformatic analysis such as identification of special domains and motifs observed in typical CYP450, homology search with BlastX program against NCBI database and phylogenetic analysis, we assumed that cloned gene might be *CYP74C* subfamily, which was known to show allene oxide synthase (AOS) or hydroperoxide lyase (HPL) activity in the oxylipin biosynthesis.

Recombinant protein encoded by cloned gene was expressed in *E. coli* using pCWori^{+} vector, and purified using Ni^{2+}-NTA column chromatography and gel filtration. This protein showed about 55 kDa in molecular weight as expected, and AOS activity resulting in final product, α- and γ- ketol from 9(S)-hydroperoxy-10(E),12(Z)-octadecadienoic acid (9-HPOD) or 13(S)-hydroperoxy-9(Z),11(E)-octadecadienoic acid (13-HPOD) substrates in the activity assay. However, it was appeared that this protein preferred more 9-HPOD than 13-HPOD as a substrate. This result indicated that purified protein might be 9-AOS in the oxylipin biosynthesis.

To identify activity swapping after changing specific residue conserved differently in AOS and HPL, phenylalanine at 100 residue (Phe100) of wild-type CYP74C was changed to leucine, and recombinant protein was expressed and purified using same condition with wild-type. Then, protein activity was measured with 9-HPOD and 13-HPOD substrates. As the result, this protein produced 9-oxononanoic acid and 12-oxo-9(Z)-dodecenoic acid,

which were known as a metabolites synthesized by HPL. In addition, 11-hydroxy-9, 10-epoxy-12(Z)-octadecenoic acid and 11-hydroxy-12, 13-epoxy-9(Z)-octadecenoic acid which were known as a product synthesized by epoxy alcohol synthase (EAS) enzyme in the oxylipin biosynthesis, were also detected. Those result indicated that phenylalanine/leucine residue may be very important to the activity of CYP74 because point-mutated CYP74C has a HPL and EAS activity in the oxylipin biosynthesis.

INTRODUCTION

Oxylipin are oxygenated natural products derived from fatty acids [1-3]. These molecules are widely spread in aerobic organisms such as mammals, flowering plants, mosses, algae, bacteria and fungi [4]. They are involved in various important biological functions, including regulation of developmental processes, responses to abiotic/biotic stress and plant defense [5-8]. Representative compounds of oxylipins are jasmonate, aldehydes, ketol, epoxides, divinyl ethers, etc [5-6,9].

Oxylipin biosynthesis initiates with the release of fatty acids from membrane lipids by the action of a lipase. The next step is an oxidation reaction by lipoxygenase (LOX) or dioxygenase to yield hydroperoxyl fatty acid (Figure 1) [10].

Hydroperoxides formed by LOXes have been shown to be relatively unstable and further metabolized by CYP74 family known as a typical cytochrome P450 [11-14].

Cytochrome P450 enzymes contain a cysteine-thiolate coordinated heme as cofactor and show absorption maximum in UV/VIS spectrum at 450 nm after reduction and CO binding [15, 17]. Typical CYP450 catalyze monooxygenase reactions via a mechanism that involves binding of oxygen to the heme iron, sequential reaction, protonation of intermediary complexes and dissociation of water [16-18].

In contrast to classical CYP450 monooxygease, the CYP74 family doesn't require molecular oxygen and an external electron donor for their catalytic activity, because they use acyl hydroperoxides as a substrate as well as an electron donor [19-20]. And allene oxide synthase (AOS) [21-26], hydroperoxide lyase (HPL) [27-29], divinyl ether synthase (DES) [30-31] and epoxy alcohol synthase (EAS) [4] are members of CYP74 family, and involved

in main branch points to produce different hydroperoxide metabolites in the oxylipin biosynthesis pathway (Figure 1). Furthermore, these enzymes catalyze isomerization rather than monooxygenation reactions [32-33].

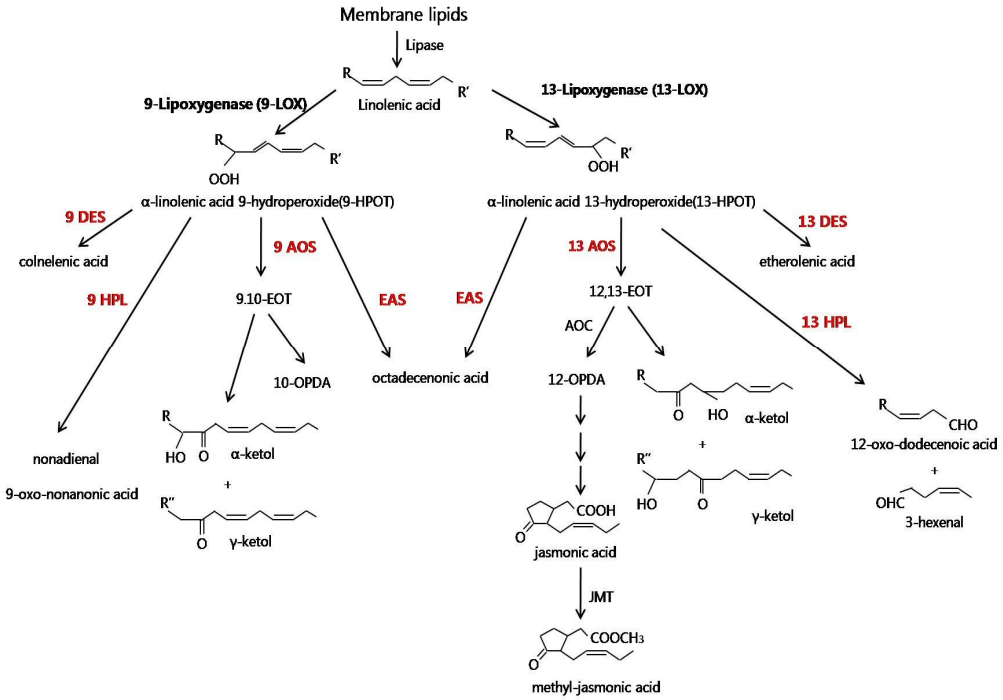

Figure 1. Oxylipin biosynthesis pathway in plants.

One of the interesting things in the activity, it is known that single point mutation in specific amino acid residue could change activity. For example, when phenylalanine in N-terminal region (137 residue) of AtAOS is changed to leucine, the enzyme activity was swapped to HPL. This publication supposes that point mutation of specific amino acid residue in CYP74 could lead activity change in main branch point of the oxylipin biosynthesis pathway [34].

AOS is related to establishing final products such as jasmonate, α-ketol, γ-ketol and 10-

OPDA [35-36], which known to be related to development, antimicrobial and/or antifungal activities [37-38]. HPL lead to formation of 9(Z)-12-oxo-9-dodecenonic acid, 3-hexenal and nonadienal, which having activities, microbes defense and predator attraction upon herbivore attack [39-46]. In the DES branch pathway, final products such as etheroleic acid and colneleic acid are produced, and these chemicals are known to be having antifungal activity [47-49]. However, DES activity is only known from a few plant species.

Recently, the diseases caused by pathogens and herbivores in grape, including Anthracnose, Gray mold, Fulgoridae and Grape phylloxera are one of the problems in its cultivation. And also climate change in the Earth can be caused to increase harmful diseases and insects.

Therefore, in order to develop critical gene increasing defense system and resistibility against harmful diseases and insects in grape, we tried to isolate *CYP74* family gene from grape and identified gene function related to oxylipin biosynthesis using recombinant protein. And also, activity swapping was tried with site-direct mutagenesis in specific amino acid residue.

MATERIALS AND METHODS

Plant material

Grape leaf (*Vitis vinifera* L.) was used as gene source to isolate *CYP74* family gene. The leaf was harvested from field at May, 2010, and stored at -80℃.

gDNA extraction

gDNA isolation was carried out with GENE ALL^{TM} Plant SV mini kit. Frozen grape leaf was ground to a fine powder quickly and completely using a mortar and pestle with liquid nitrogen. Around 100 mg of ground tissue was used to extract gDNA. Extraction procedure was followed by manufacturer's instructions.

gDNA-PCR for gene cloning

Specific primers were designed based on sequence information of grape *CYP74* family genes that are registered in NCBI. The forward primer liked with some nucleotides coding MAKKTSS peptide segment in N-terminal region to improve recombinant protein expression in *E.coli*. And some nucleotides coding 5-histidine residues in C-terminus were added in reverse primer to purify the protein using Ni^{2+}-NTA affinity column chromatography.

Primer sequences used for amplifying target gene were as below; forward primer 5' - GGA GTA CATATG GCT AAG AAA ACG TCA TCC TCG TCT TCT TCT TCT- 3' and reverse primer 5' - GTT AAT GTC GAC TCA GTG GTG GTG GTG GTG AGT GTA ACT GGT CTT GGT- 3'.

gDNA-PCR amplification was performed using Ex-Taq™ DNA polymerase (Takara, Japan). Composition of reaction mixture and thermal cycling parameters are described in Table 1. The PCR product was separated on 1.0% agarose gel and stained with ethidium bromide. The target DNA of each PCR product was extracted from agarose gel using QIAquick Gel Extraction kit (Qiagen, USA) and ligated into the yT & A vector (Figure 2). And the plasmid was transformed into TOP10 competent cell.

Table 1. PCR mixture and thermal cycling program for cloning *CYP74* family gene from genomic DNA of grape

PCR mixture (μℓ)		Thermal cycling program	
Template gDNA (ng/μℓ)	1	Initial activation step	95℃10 min
Forward primer (10 pmol/μℓ)	1	Denaturation Annealing Extention	95℃ 40 sec 43℃ 50 sec 72℃ 1 min 40 sec
Reverse primer (10 pmol/μℓ)	1		
dNTP (2.5 mM each)	2	Number of cycles	5 times cycle
10xPCR reaction buffer	2	Denaturation Annealing Extention	95℃ 40 sec 50℃ 50 sec 72℃ 1 min 40 sec
Ex-Taq polymerase (unit/μℓ)	0.2		
Sterile dH_2O	7.2	Number of cycles	30 times cycle
Total volume	20	Final cycle extention	72℃ 10 min

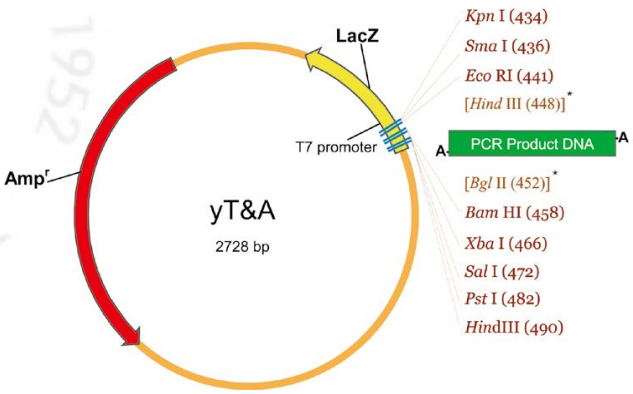

Figure 2. Vector map of yT&A for cloning PCR product.

Sequence analysis

Sequence identification of cloned genes were ordered to company "Bionics" (Seoul, Korea), and primers used for sequencing reaction were M13 forward and reverse primers.

After sequence analysis, open reading frame and deduced amino acid sequences were identified by CAP3 assemble program (http://pbil.univ-lyon1.fr/cap3.php) and ExPASY translation tool (http://web.expasy.org/translate/). Homology search was carried out with BlastX program in the NCBI. And phylogenetic relationship was analyzed by ClustalX and Tree View program.

Construction of *E.coli* expression vector

For recombinant protein expression in *E.coli*, pCWori$^+$ vector was used and the map of this plasmid was described in Figure 3. To ligate target gene into expression vector, the plasmid, pCWori$^+$, was digested with *Nde* I and *Sal* I restriction enzymes. And also the recombinant plasmid containing grape *CYP74* family gene was digested with same

restriction enzymes. Then, digested expression vector and target gene were ligated using Rapid DNA Ligation kit (Roche, Germany) according to manufacturer's instructions.

Ligated plasmid was transformed into TOP10 cell to amplify plasmid and analyze sequence. Collected construct identified after sequencing was used for transformation of expression cell.

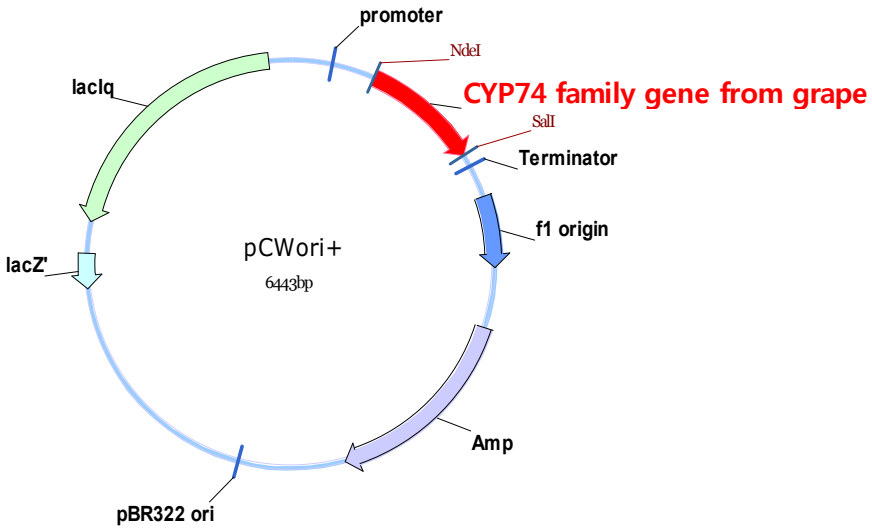

Figure 3. Vector map of pCWori^{+} for expressing *CYP74* family gene in *E. coli*.

Site-directed mutagenesis

To obtain plasmid containing point-mutated *CYP74* family gene, site-specific primers were designed to change amino acid sequence from phenylalanine to leucine (F100L), and synthesized. The primer sequences were as below; forward primer 5' – GTC GAG AAG AGA AAC GTC TTG GTC GGG ACT TTC ATG CCC- 3' and reverse primer 5' –GGG CAT GAA AGT CCC GAC CAA GAC GTT TCT CTT CTC GAC- 3'. Then, site-directed mutagenesis was carried out by PCR. Components of PCR and thermal cycling program were described in Table 2.

To remove the template DNA, 1.5 ㎕ of *DpnI* restriction enzyme was treated into PCR

product and mixture was incubated for 90 min at 37℃. Then, plasmid was transformed into TOP10 cell to amplify plasmid and analyze sequence. And collected construct identified after sequencing was used for transformation of expression cell.

Table 2. PCR mixture and thermal cycling program for site-direct mutagenesis

PCR mixture (㎕)		Thermal cycling program	
Template DNA (ng/㎕)	2	Initial activation step	95℃ 2 min
Forward primer (10 pmol/㎕)	1.5	Denaturarion	95℃ 30 sec
Reverse primer (10 pmol/㎕)	1.5	Annealing	55℃ 1 min
dNTP (2.5 mM each)	2	Extention	72℃ 7 min 30 sec
10xPCR reaction buffer	5		
pfu polymerase (unit/㎕)	1.5		
Sterile dH_2O	38	Number of cycles	20 times cycle
Total volume	50	Final cycle extention	72℃ 10 min

Transformation of plasmid into *E.coli* competent cell

The $CaCl_2$-treated cells were taken out from -70℃, and thawed in ice. After adding 5 ㎕ ligation mix to the cells, the tube were swirled and placed on ice for 30 min. And then the cells were heated shock by placing tubes for 45 sec in 42℃ water bath. Immediately the tube was placed on ice for 5 min. After that, 1 ml LB medium was added to tube and then incubated for 1 hr at 37℃. The cells were spined down for 5 min at 13,000 rpm. After discard most of the media, the cells were resuspended and smeared to the LB plate containing appropriate antibiotics, then incubated 12 to 16 hr at 37℃ or overnight. A single

colony was picked out and transferred into single 5 ml of LB liquid medium containing appropriate antibiotics. And the stock cells were prepared with 15% glycerol and stored at -70℃.

Expression of recombinant protein

Seed culture was carried out first before induction culture. Cell taken out from cell stock at -70℃ was inoculated into 30 ml of TB broth containing appropriate antibiotics. Then, the culture was incubated at 37℃ for overnight with shaking about 180 rpm. For small scale expression test, 2 ml of seed culture cell was inoculated into 50 ml of TB broth containing appropriate antibiotics and heme precursor (δ-ALA), which is usually known to improve the yield of spectrally active P450, then incubated at 37℃ for 2~3 hrs with shaking about 200 rpm until 0.6~0.8 of OD_{600}. Gene expression was induced by adding IPTG to media to a final concentration of 0.7 mM, and the culture was incubated for 2 days at 27-28℃ with shaking 120 rpm.

For large scale expression, 30 ml of seed culture cell was inoculated into 800 ml of TB broth containing appropriate antibiotics and heme precursor (δ-ALA) then incubated at 37℃ for 2~3 hrs with shaking about 200 rpm until 0.6~0.8 of OD_{600}. Gene expression was induced by adding IPTG to media to a final concentration of 0.7 mM, and the culture was incubated for 2 days at 27-28℃, 120 rpm.

Extraction of recombinant protein

After 2 days, the cells were harvested from 800 ml liquid culture by centrifugation at 5,000 rpm for 12 min. The cell pellet was suspended in 60 ml Ni^{2+}-NTA washing buffer (lysis buffer) containing DNase and 1.2% O.G (octyl-β-D-glucopyranoside), and incubated with gentle stirring on magnetic stir for 2-3 hrs at 4℃. Then, the cells were lysized by sonication (10 sec pulse, 50 sec resting for 7 min, on ice), and incubated again with gentle stirring on magnetic stir for overnight at 4℃. The protein was obtained through centrifuging (15,000 rpm for 1 hour, 4℃). Supernatant was used for purification of recombinant protein.

Purification of recombinant protein

Ni^{2+}-NTA resin was used to purify the recombinant protein using its His-tag. The column was pre-washed with 50 ml lysis buffer. The protein was applied to the column. Then, column was washed with 50 ml of lysis buffer containing 0.5% O.G, and followed by 50 ml of lysis buffer containing high salt (1 M NaCl), 50ml of lysis buffer containing 0.1% O.G and 20 mM imidazole and 70 ml lysis buffer containing 0.1% O.G and 50 mM imidazole. The target protein was eluted by fractionation with 50 ml of lysis buffer containing 0.1% O.G and 200 mM imidazole.

The fraction containing target protein was selected by UV spectrophotometric analysis and SDS-PAGE. The best fraction were combined and centrifuged at 5,500 rpm for 40 min using Millipore tube. Further, the fraction was purified by gel filtration with AKTA prime plus equipped with Superdex 200 column. Column was pre-equilibrated by 50 ml of running buffer containing 0.1 M Tris-HCl (pH7.3), 0.3 M NaCl and 15% glycerol, and protein was fractionated with same buffer for 4 hrs. The fraction containing target protein was selected by UV spectrophotometric analysis and SDS-PAGE for further study.

Table 3. Gel filtration condition for size-fractionation of recombinant protein.

Break point	Volume	Flow	Fraction	Buffer	Injection	Autozero
1	0.0	0.5	0.0	1	Load	N
2	10.0	0.5	0.0	1	Inj	Y
3	13.0	0.5	0.0	1	Load	N
4	40.0	0.5	1.0	1	Load	N
5	130.0	0.5	0.0	1	Load	N
6	190.0	0 .5	0.0	1	Load	N

SDS-PAGE

Expression and purification of recombinant protein were detected by SDS-PAGE on 10~12% gel. Protein sample was mixed with SDS-PAGE sample buffer (5X) and heated at 95℃ for 10 min. Sample was loaded into wells and run until the bromophenol blue dye reaches to the bottom edge.

Visualization of protein bands was carried out by Coomassie staining, and destaining was done using solution containing 10% methanol and 10% acetic acid.

P450-CO complex assay

Purified protein was diluted Kpi buffer and reduced by adding 10 ㎕ of 0.5 M sodium hydrosulfite. Immediately, CO gas was allowed to flow into the sample for 10~20 sec. Then, UV/VIS absorption from 250 to 600 nm was scanned by spectrophotometer.

Analysis of recombinant protein activity

Two kinds of chemicals, 9(S)-hydroperoxy-10(E),12(Z)-octadecadienoic acid (9HPOD) and 13(S)-hydroperoxy-9(Z),11(E)-octadecadienoic acid (13HPOD), were used as substrate for enzyme reaction. Purified protein was incubated with each substrate (200 μM) at 23℃ for 15 min. Part of the reaction product was treated with 3 vol of 30 mM O-methylhydroxylamine in methanol at 23°C for 2 h to generate O-methyloxime derivatives of short-chain aldehydes and other carbonyl-containing oxylipins. Additional derivatization of products extracted with diethyl ether was performed by consecutive treatments with ethereal diazomethane and a 2:1:2 (vol/vol/vol) mixture of trimethylchlorosilane, hexamethyl-disilazane and pyridine to generate methyl esters from carboxylic acids and trimethylsilyl ethers from alcohols, respectively.

Oxylipin profiles generated from the incubation of hydroperoxides with CYP74 enzymes were determined by GC–MS analysis run in the scan mode (m/z 50–600) and using the authentic compounds as references (Lipidox Co.). The selected ion monitoring (SIM) mode was used for sensitive and specific detection.

Prediction of three-dimensional protein structure

A three-dimensional (3-D) model of point-mutated VvCYP74 was built using the Swiss protein modeling server [50]. The crystal structure of (AtAOS F137L; Protein Data Bank ID 3dskA) was used as a modeling template. Structural visualization was performed using PyMOL (www.pymol.org) [51].

RESULTS AND DISCUSSION

I. Cloning of *VvCYP74* gene and characterization of its recombinant protein

Cloning of *CYP74* family gene from *Vitis vinifera* L.

Genomic DNA (gDNA) was extracted from grape leaf, and its quality was checked by agarose gel electrophoresis. Extracted gDNA made clear band in the gel with over 10 kb as shown in Figure 4A. There was not any sign of degraded DNA. Concentration of the gDNA was measured by spectrophotometer and 240 ng/㎕ of gDNA was used for cloning target gene.

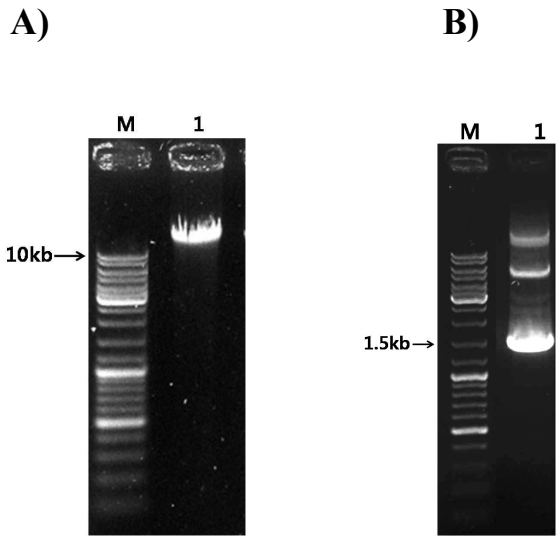

Figure 4. Agarose gel electrophoresis regarding *CYP74* family gene cloning from *V. vinifera* L. (A) Genomic DNA extracted from grape leaf, (B) Amplified DNA using specific primer of *CYP74* family gene by gDNA-PCR, M: marker ladder.

A gDNA PCR was carried out with specific primer and PCR product was separated on agarose gel. As the result, DNA band of expected size, around 1.5 kb, was observed in the gel after staining with ethidium bromide (Figure 4B). So, DNA in the band was extracted from the gel and ligated into the yT&A vector for sequencing, and then ligated plasmid was transformed into TOP10 competent cell. Correct colony containing target gene was identified by colony PCR with same primers in the PCR cloning and used for plasmid amplification and purification . Purified plasmid was used for sequence analysis.

Bioinformatic analysis of cloned gene

Nucleotide sequences were obtained after sequencing cloned gene, and its length was identified as 1452 bp in the open reading frame, which encoded 483 amino acid residues.

Deduced amino acid sequences contained specific domains and motifs, which conserved in CYP450. Each domain and motif were indicated in Figure 4. Heme-binding domain was observed in 432~441 regions as NKQCSGKDLV amino acid sequences, and contained cysteine residue forming the proximal heme ligand. I-helix central domain (IHCD) was also detected in this sequence as LVFLAGFNSFGGMKV amino acid sequences. Two motifs, PPGP and EXLR, were located in 65~68 and 345~348 residues, respectively (Figure 5).

Homology search was also carried out to assume putative function of cloned gene by blastX program in the NCBI. As the result, cloned gene was highly homologous with other *CYP74* family genes isolated from plants such as *Vitis vinifera*, *Prunus dulcis*, *Cucumis sativus*, *Salua pennellill* and *Lotus japonia*. Identities between cloned gene and other genes were more than 60%. Multi-alignment was shown in Figure 6.

Taken those two results, it was assumed that cloned gene might be CYP450 gene and belonging to *CYP74* family. So, to guess subfamily of this gene, phylogenetic analysis was

performed by comparing known *CYP74* family genes, including A, B, C and D subfamilies. As the result, it was recognized that cloned gene was classified to CYP74C subfamily gene, which was known to be functioning as HPL or AOS enzyme in the oxylipin biosynthesis pathway (Figure 7).

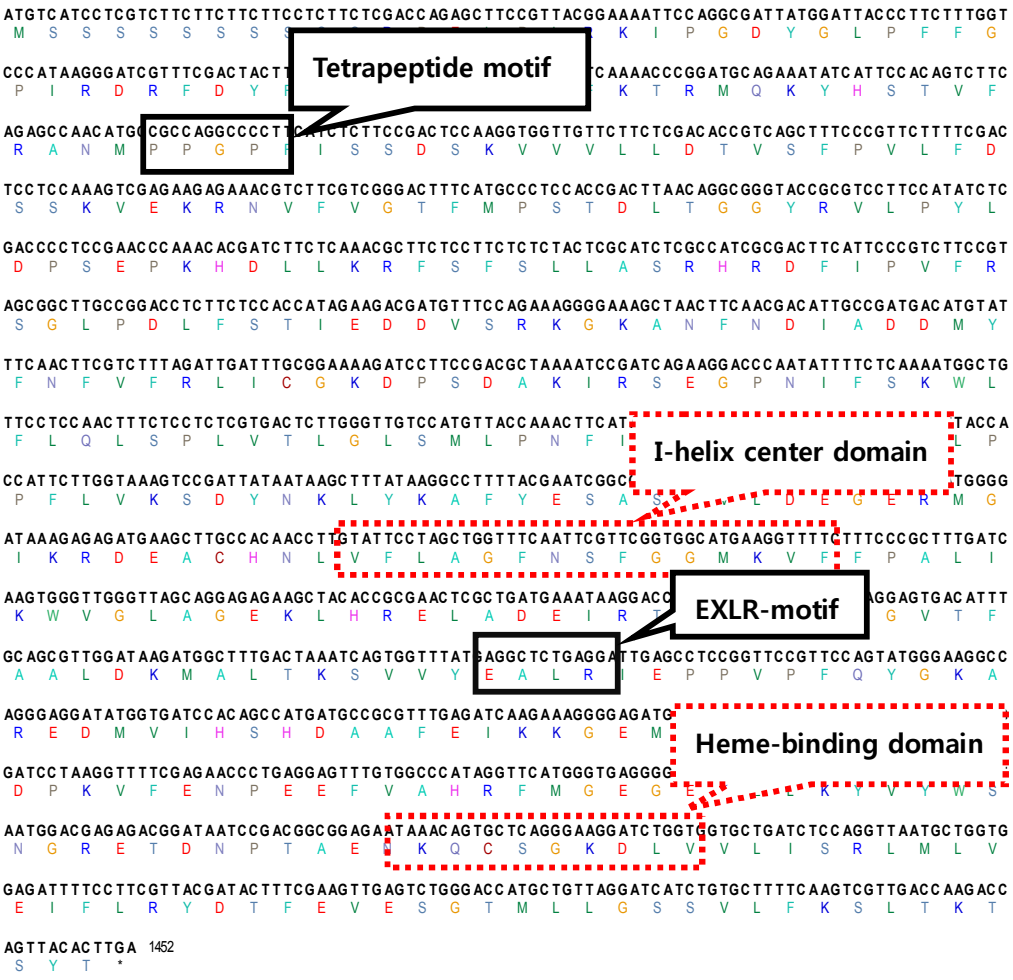

Figure 5. Nucleotide and deduced amino acid sequences of *CYP74* family gene isolated from *V. vinifera* L. The nucleotide sequences had a 1452 bp open reading frame, which encoded a 483 amino acid residues. Red dot box indicated two domains, I-helix center domain and heme-binding domain, and black line box denoted two motif, tetrapeptide modif and EXLR motif. The stop codon was indicated by an asterisk.

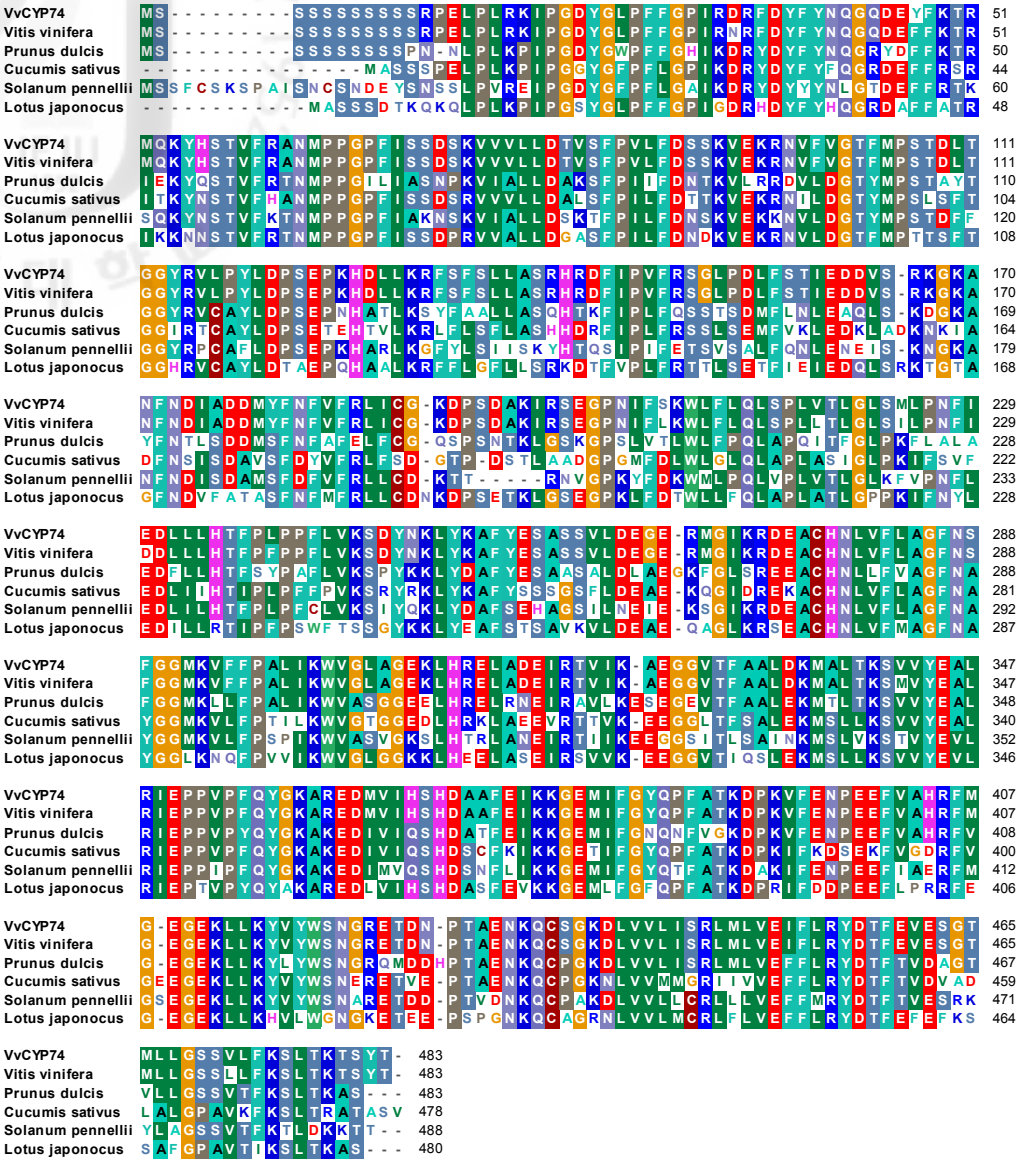

Figure 6. Alignments of the deduced amino acid sequences of *CYP74* family gene isolated from *Vitis* spp and other plants. Amino acid sequences were aligned using ClustalX 1.83.

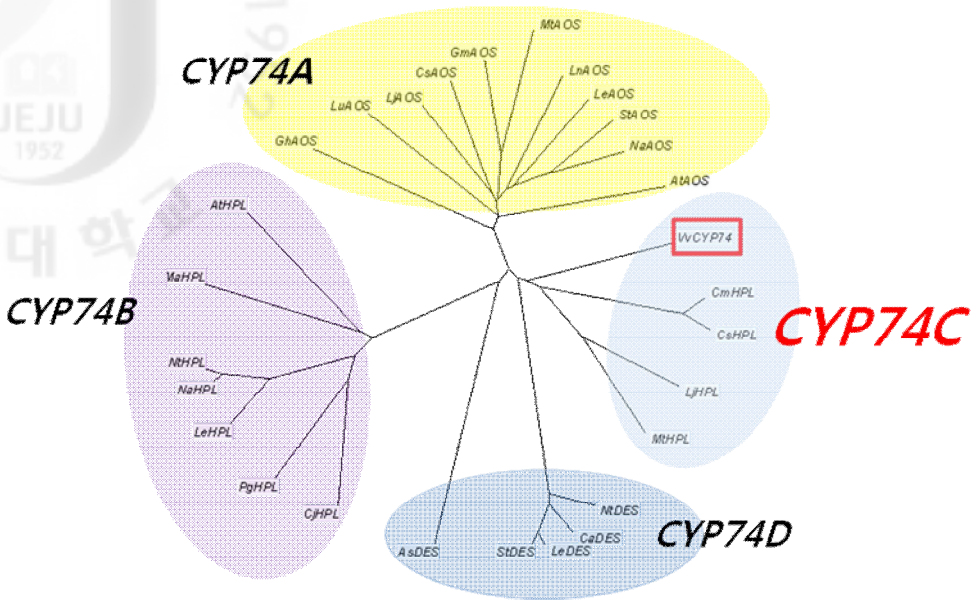

Figure 7. Phylogenetic analysis of *CYP74* family gene isolated from *Vitis* spp. and other plants. Phylogenetic tree was generated by ClustalX and Tree View program.

Protein expression in *E.coli*

Protein expression vector in *E. coli* was constructed with pCWori^{+}, which was frequently used for expressing CYP450 gene in *E. coli*. To ligate gene into pCWori^{+}, gene was amplified with new primers containing specific enzyme recognition site, *NdeI* and *SalI*, because both two sites were no exist within cloned gene but in the multi-cloning site of expression vector. Cut both PCR product and vector was ligated and then transferred into TOP10 cell.

Collect colony was checked by PCR and sequences in ligated expression vector was confirmed by sequencing (Figure 8A). Then, constructed expression vector was transformed into an *E. coli* expression cell, including DH5α/pGro12, pLysS and C41a. Transformant was

confirmed by colony PCR, and then used for protein expression (Figure 8B).

To check the gene expression, small-scale test, 30 ml culture, was carried out with various expression cells, and recombinant protein was checked by SDS-PAGE. As the results, it was supposed that DH5α/pGro12 cell was more suitable to express target gene than others. As shown in Figure 9A, expected band, about 55 kDa protein, was observed in soluble fraction, although the inclusion body of this protein was also formed a little in this condition.

In large-scale test (800 ml culture), similar result with small-scale test was appeared that recombinant protein corresponding to about 55 kDa was observed in soluble fraction (Figure 9B).

Those results indicated that induction condition and cell used for those experiments might be applied to produce the recombinant proteins for our target gene.

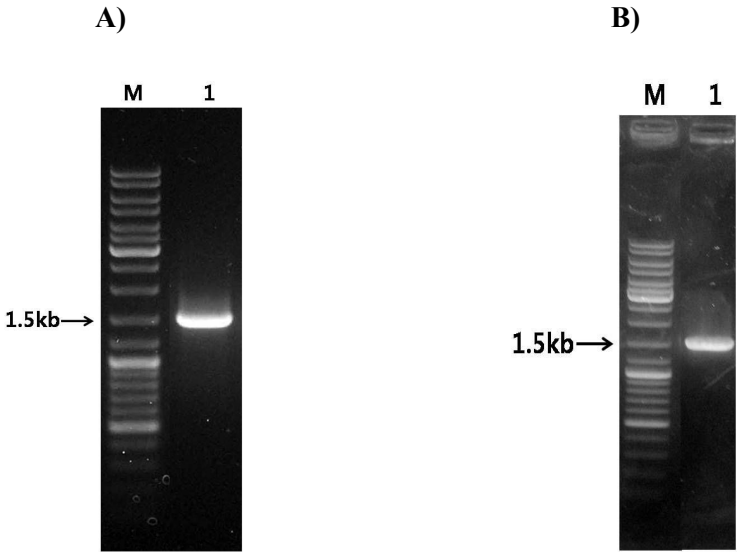

Figure 8. Agarose gel electrophoresis amplified DNA from transformants. (A) *VvCYP74* family gene in TOP10, (B) *VvCYP74* family gene into DH5α/pGro12. M: marker ladder.

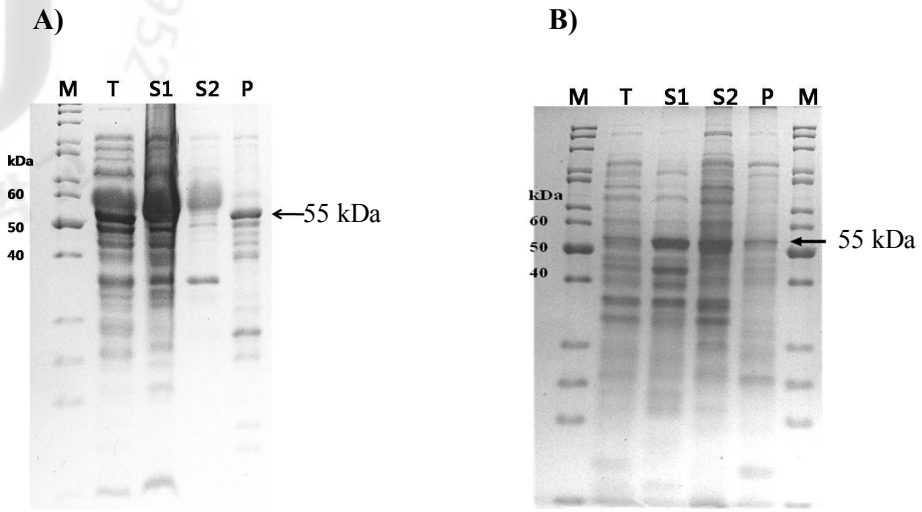

Figure 9. SDS-PAGE of recombinant protein extracted from *E.coli*, DH5α/pGro12, using BugBuster® Protein Extraction Reagent. A SDS-PAGE was stained with Coomassie Brilliant Blue R250. Molecular mass (kDa) of standard proteins was shown on the left and/or right. T: crude cell extracts, S1, S2: supernatant, P: pellet. (A) small-scale expression test with 30 ml of TB broth, (B) Large-scale protein expression with 800 ml of TB broth. The arrow indicated the expected protein band in 55 kDa molecular weight.

Purification of recombinant protein from *E.coli*

To express and purify the recombinant protein, large-scale induction culture was performed in the optimized condition, and protein was purified by Ni^{2+}-NTA affinity column chromatography followed by gel filtration. Thereafter, each fraction was checked by SDS-PAGE.

The result was shown in Figure 10A and 11A. Major fractions on affinity chromatography contained the expected 55 kDa band as the main protein component, and pure protein was obtained after gel filtration.

To identify spectroscopic characteristics for eluted protein, UV/VIS spectrum was measured on range from 250 to 600 nm, and shown in Figure 10B and 11B. In the spectrum, maximum absorption was ranged from 390 to 420 nm and also detected 535 and 575 nm absorption, which is known to be characteristics of the typical absorption spectrum of CYP450 without reduction and CO binding.

Those result supposed that purified protein was derived from target gene expression and might be CYP450.

A) B)

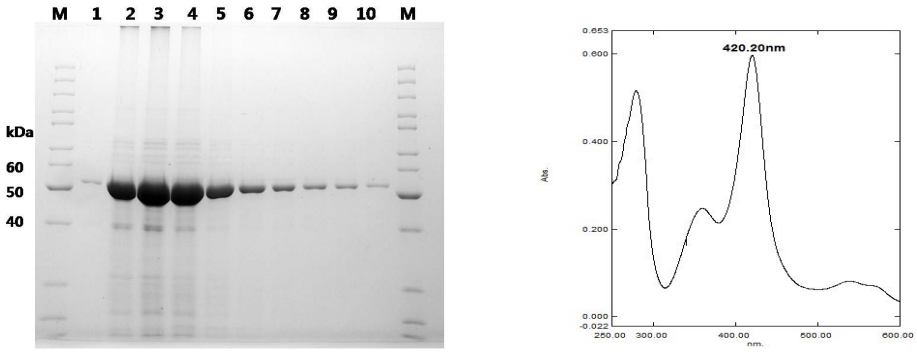

Figure 10. SDS-PAGE and UV/VIS spectrum of fractionated protein by affinity column chromatography. (A) SDS-PAGE. Gel was stained with Coomassie Brilliant Blue R250. Molecular mass (kDa) of standard proteins was shown on the left and right. The main fractions contained the expected 55 kDa band as the major protein component. (B) UV/VIS spectrum. Purified protein showed λ_{max} at 420 nm.

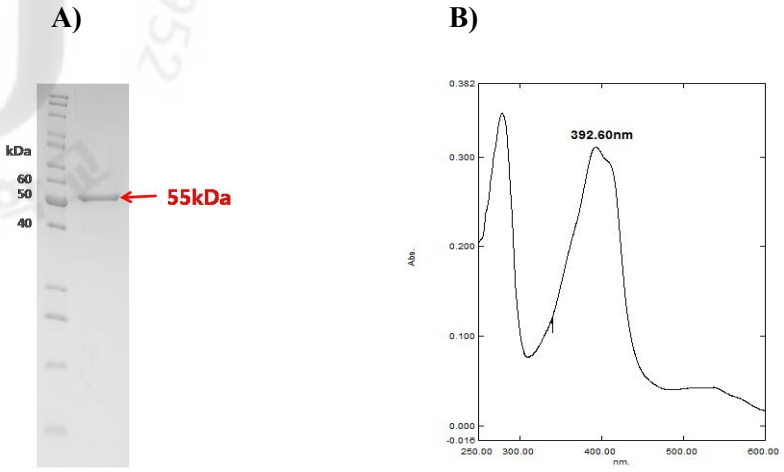

Figure 11. SDS-PAGE and UV/VIS spectrum of fractionated protein by gel filtration. (A) SDS-PAGE. Gel was stained with Coomassie Brilliant Blue R250. Molecular mass (kDa) of standard proteins was shown on the left. Combined best fraction shown the single band corresponding to 55 kDa molecular weight. (B) UV/VIS spectrum. Purified protein showed λ_{max} at 392 nm.

Spectroscopic characterization of recombinant protein

Although purified protein was assumed that it might be CYP450 by UV/VIS scanning, we tried to confirm that it was CYP450 with CO difference spectrum, because typical CYP450 is known to show a soret peak at 450 nm after reduction of iron ion and binding CO to this site. As the result, maximum absorption was shifted from 420 nm to 442 nm (Figure 12).

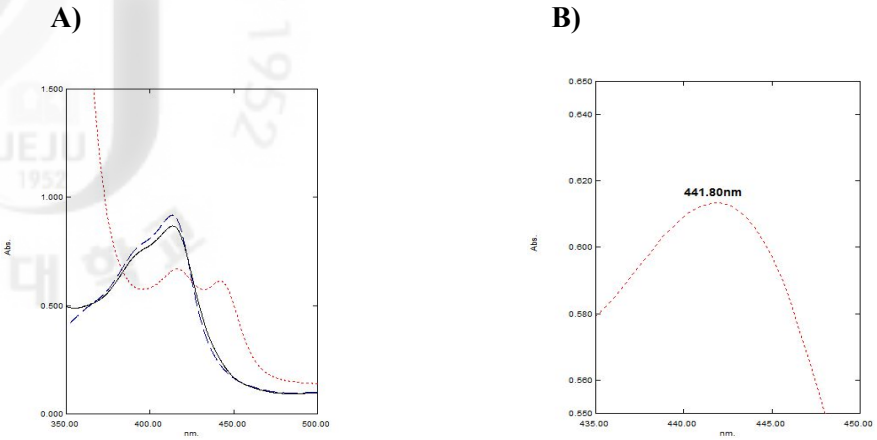

Figure 12. CO difference spectrum of recombinant protein. (A) UV/VIS spectrum of recombinant protein before and after treatment of reductant and CO gas. Solid-black line: No treatment of reductant and CO gas, Dashed-blue line: Treatment of only redundant, Dotted-red line: Treatment of both reductant and CO gas. (B) Magnified view of the spectrum after treatment of both reductant and CO gas. Soret peak was at 441 nm.

Analysis of recombinant protein activity

To identify the protein activity, 9HPOD and 13HPOD were used as substrate and reacted with purified protein. Then a product of enzyme reaction was detected by GC/MS.

As the result, two compounds, α-ketol and γ-ketol which were known as a product synthesized by AOS enzyme in the oxylipin biosynthesis, were detected in both reactions. However, 9HPOD was appeared as more a preferable substrate than 13HPOD (Figure 13). This result meant that the purified protein has a 9AOS activity in the oxylipin biosynthesis.

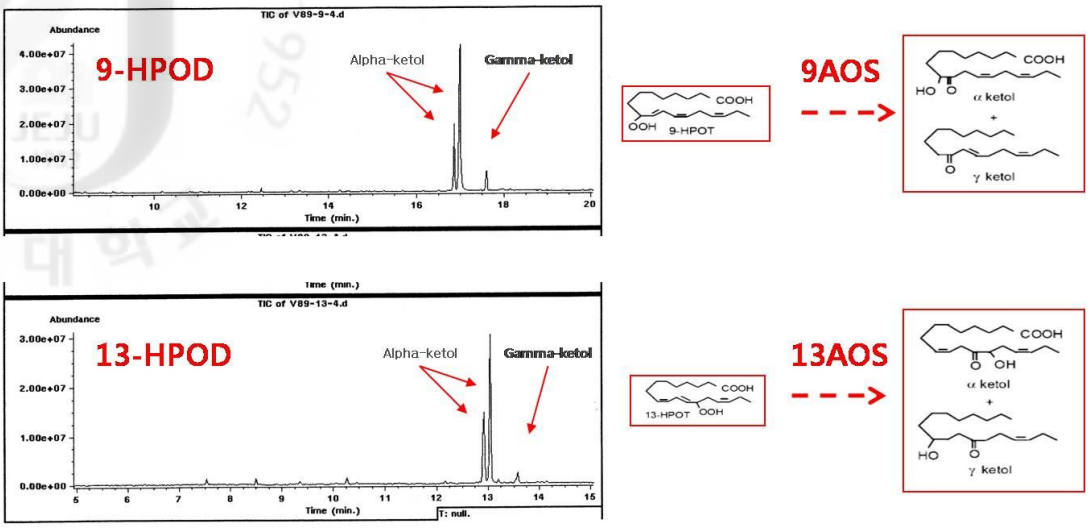

Figure 13. Chromatogram for reactant of purified protein and substrate analyzed by GC/MS. Upper: 9HPOD substrate, Lower: 13HPOD, arrow indicated two products, α-ketol and γ-ketol.

II. Site-direct mutagenesis of *VvCYP74* gene and characterization of its recombinant protein.

Site-direct mutagenesis

To change the phenylalanine (Phe100) in the active site to leucine, whole pCWori^{+} vector containing wild-type *VvCYP74* gene was amplified with primers to allow changing TTG to TTC. And change of nucleotide and deduced amino acid sequences were identified by sequencing as shown in Figure 14. Then, this vector was directly used to express a recombinant protein.

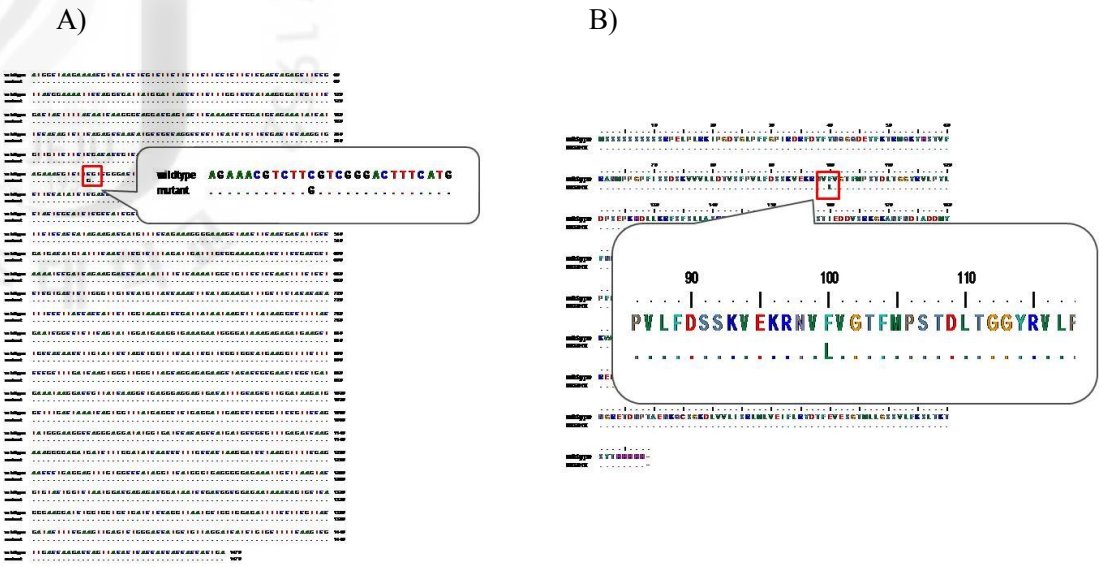

Figure 14. Graphical representation of changed nucleotide and amino acid sequence in wild-type *VvCYP74*. (A) Nucleotide sequence, (B) Amino acid sequence.

Protein expression for site-mutated gene in *E.coli*

Protein expression vector, pCWori^{+} harboring site-mutated gene, was transformed into DH5α/pGro12. Transformant was confirmed by colony PCR, and then used for protein expression (Figure 15).

To check the gene expression, small-scale test (30 ml culture), was carried out with same condition for wild-type *VvCYP74* gene expression, and recombinant protein was checked by SDS-PAGE (Figure 16). As the results, soluble protein corresponding to about 55 kDa was observed, although an inclusion body of this protein was also formed a little in this condition. So, large-scale expression (800 ml culture) was performed using those conditions to purify a recombinant protein.

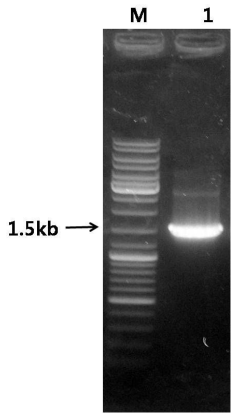

Figure 15. Agarose gel electrophoresis of amplified DNA from transformants, DH5α/pGro12. M: marker ladder.

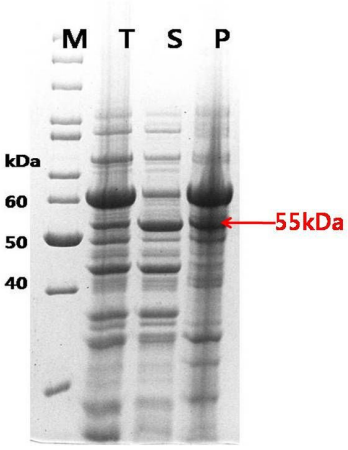

Figure 16. SDS-PAGE of recombinant protein extracted from *E.coli*, DH5α/pGro12, using BugBuster® Protein Extraction Reagent. A SDS-PAGE was stained with Coomassie Brilliant Blue R250. Molecular mass (kDa) of standard proteins was shown on the left and/or right. T: crude cell extracts, S: supernatant, P: pellet. The arrow indicated the expected protein band in 55 kDa molecular weight.

Purification of recombinant protein from *E.coli*

Recombinant protein was purified by Ni^{2+}-NTA affinity column chromatography followed by gel filtration. After that each fraction was checked by SDS-PAGE.

As the result, major fractions after Ni^{2+}-NTA affinity column chromatography contained the expected 55 kDa band as the main protein component, and pure protein was obtained after gel filtration.

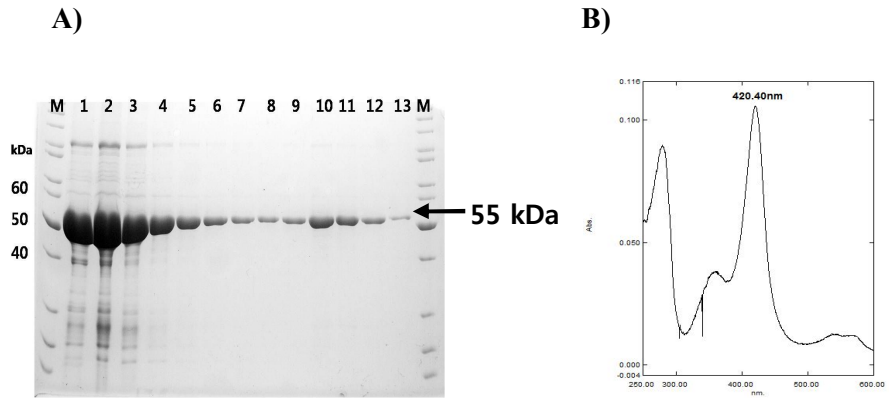

Figure 17. SDS-PAGE and UV/VIS spectrum of fractionated protein by affinity column chromatography. (A) SDS-PAGE. Gel was stained with Coomassie Brilliant Blue R250. Molecular mass (kDa) of standard proteins was shown on the left and right. The major fractions contained the expected 55 kDa band as the main protein component. (B) UV/VIS spectrum. purified protein showed λ_{max} at 420 nm.

To identify spectroscopic characteristics for the eluted protein, UV/VIS spectrum from 250 to 600 nm was measured, and shown in Figure 17B and 18B. In the spectrum, maximum absorption was ranged from 390 to 420 nm and also detected 535 and 575 nm absorption,

which is known to be characteristics of a typical absorption spectrum of CYP450 without reduction and CO binding.

Those result supposed that purified protein was derived from target gene expression and might be CYP450.

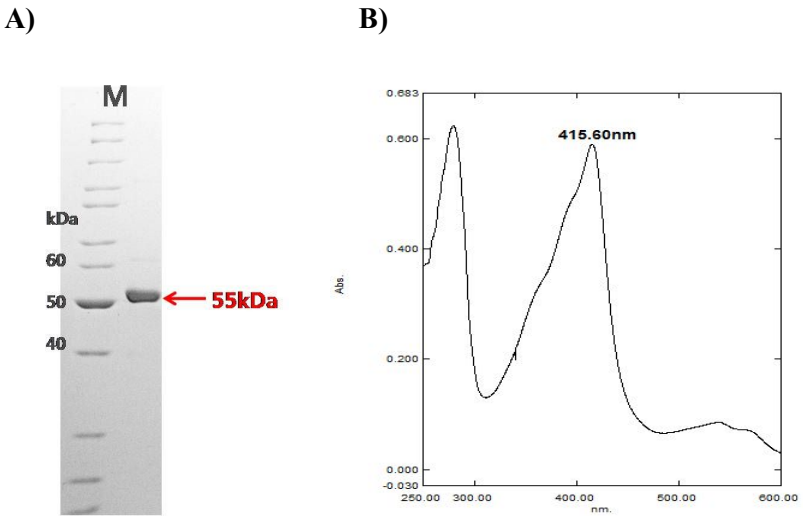

Figure 18. SDS-PAGE and UV/VIS spectrum of fractionated protein by gel filtration. (A) SDS-PAGE. Gel was stained with Coomassie Brilliant Blue R250. Molecular mass (kDa) of standard proteins was shown on the left. Combined best fraction was shown the single band corresponding to 55 kDa molecular weight. (B) UV/VIS spectrum. purified protein showed λ_{max} at 415 nm.

Spectroscopic characterization of recombinant protein

Although purified protein was assumed that it might be CYP450 by UV/VIS scanning, we tried to confirm that it was CYP450 with CO difference spectrum, because typical CYP450 is known to show a soret peak at 450 nm after reduction of iron ion and binding CO to this site. As the result, maximum absorption was shifted from 420 nm to 444 nm (Figure 19).

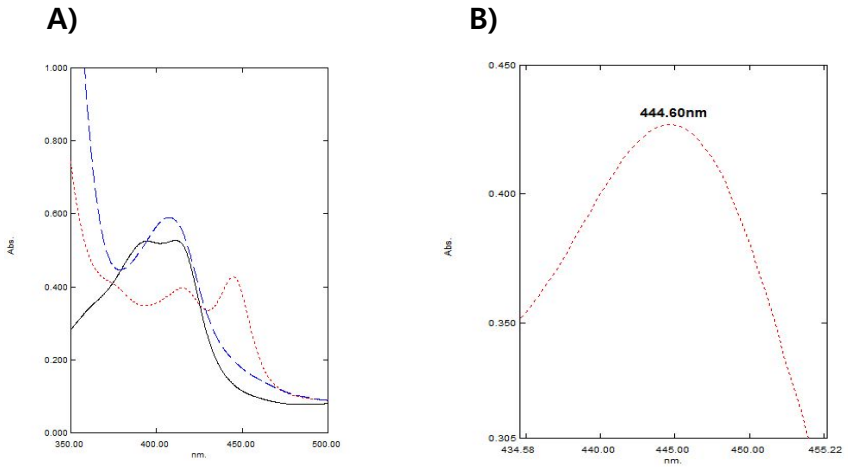

Figure 19. CO difference spectrum of recombinant protein. (A) UV/VIS spectrum of recombinant protein before and after treatment of reductant and CO gas. Solid-black line: No treatment of reductant and CO gas, Dashed-blue line: Treatment of only redundant, Dotted-red line: Treatment of both reductant and CO gas. (B) Magnified view of a spectrum after treatment of both reductant and CO gas. Soret peak was at 444 nm.

Analysis of recombinant protein activity

To identify the protein activity, 9HPOD and 13HPOD were used as substrate and reacted with purified protein. Then a product of enzyme reaction was detected by GC/MS.

As the result, two compounds, 9-oxononanoic acid and 12-oxo-9(Z)-dodecenoic acid

which were known as a product synthesized from 9HPOD and 13HPOD by HPL enzyme in the oxylipin biosynthesis, were detected respectively. In addition, 11-hydorxy-9, 10-epoxy-12(Z)-octadecenoic acid and 11-hydorxy-12, 13-epoxy-9(Z)-octadecenoic acid which were known as a product synthesized from 9HPOD and 13HPOD by EAS enzyme in the oxylipin biosynthesis, were also detected (Figure 20).

Those result indicated that point-mutated VvCYP74 has a HPL and EAS activity in the oxylipin biosynthesis, and phenylalanine/leucine residue may be very important to the activity of this CYP74 isolated from Grape.

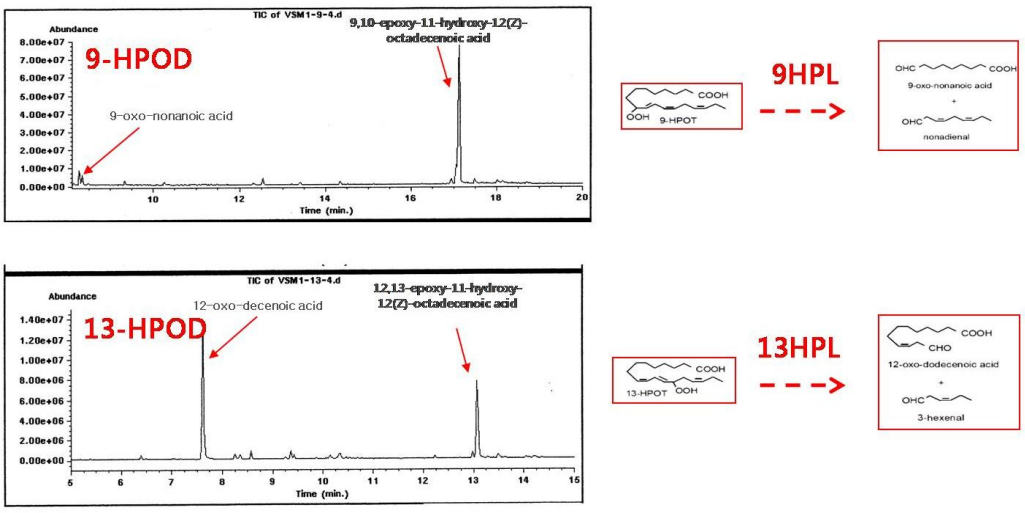

Figure 20. Chromatogram for reactant of purified protein and substrate analyzed by GC/MS. Upper: 9HPOD substrate, Lower: 13HPOD, arrow indicated HPL and EAS products, 9-oxononanoic acid, 12-oxo-9(Z)-dodecenoic acid, 11-hydorxy-9, 10-epoxy-12(Z)-octadecenoic acid and 11-hydorxy-12, 13-epoxy-9(Z)-octadecenoic acid.

Three-dimensional structure of point-mutated VvCYP74

As shown in figure 21A, predicted three-dimensional structure of point-mutated VvCYP74 showed typical structure of CYP450 harboring heme-binding domain, helix-rich side and beta-sheet-rich side. Heme-binding domain oriented nearly parallel to the surfaces between the L and I helices, and helix and beta-sheet were rich on the right and left sides, respectively.

When heme-binding pocket was magnified to identify the point-mutated residue in the structure, leucine, mutated residue from phenylalanine, was observed on nearby heme-pocket (Figure 21B). This result supposed that phenylalanine/leucine existing on nearby heme-pocket might be having essential role to convert substrate.

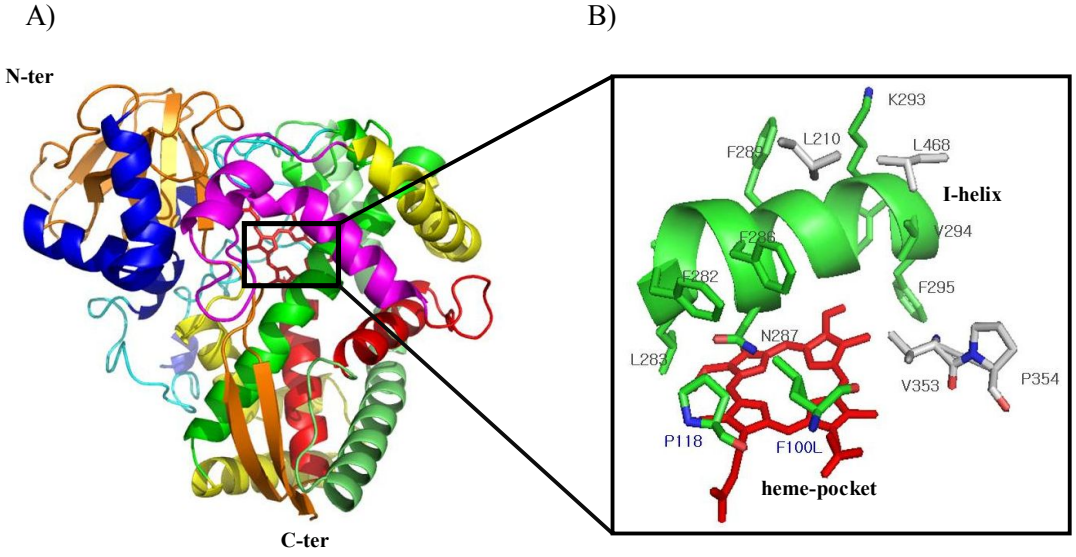

Figure 21. Predicted three-dimensional protein structure of point-mutated VvCYP74. (A) Whole sturucture. Structrue was drawn as rebbon diagram, and shown with rainbow-color from N terminus to C terminus. (B) Magnified structure of heme-pocket. F100L indicated point-mutated amino acid residue.

CONCLUSION

In this study, *CYP74* gene was isolated from grape, *Vitis vinifera* L, and characterized using recombinant protein expressed in and purified from *E.coli*. Isolated gene from grape was assumed as CYP74C subfamily through bioinformatic analysis. Recombinant protein encoded by this gene showed AOS activity to produce α- and γ- ketol from 9HPOD or 13HPOD substrates in the activity assay.

To control the activity of wild-type CYP74C in grape, Phe 100 residue in CYP74C was changed to leucine by site-direct mutagenesis, and recombinant protein was expressed and purified using same procedure used in CYP74C. In the activity assay, this mutated CYP74C (F100L) appeared both HPL and EAS activities.

These results indicated that wild-type CYP74C isolated through this study might be having AOS activity, and phenylalanine and leucine as a critical residues in the catalytic site, might be a very important residues in the enzyme functions, AOS and HPL, respectively.

Consequently, isolated CYP74C and its point mutant were identified as having activities to regulate oxylipins in grape. So, this genes' information and its activities will be useful to develop new cultivar having resistibility against harmful diseases and insects in grape.

REFERENCES

1. Graveland, A. Enzymatic oxidations of linoleic acid and glycerol-1-monolinoleate in doughs and flour-water suspensions. J Am Oil Chem Soc 47:352–361(1970)

2. Wang, X., Devaiah, S. P., Zhang, W., Welti, R. Signaling functions of phosphatidic acid. Prog Lipid Res **45**, 250–7(2006)

3. Xue, H., Chen, X., Li, G. Involvement of phospholipid signaling in plant growthand hormone effects. Curr Opin Plant Biol **10**, 483–9(2007).

4. Andreou, A., Brodhun, F., Feussner, I. Biosynthesis of oxylipins in non-mammals. Prop. Lipid Res. **48**,148-170(2009)

5. Ble´e, E. Phytooxylipins and plant defense reactions. Prog. Lipid Res. **37**, 33–72(1998).

6. Grechkin, A. N. Recent developments in biochemistry ofthe plant lipoxygenase pathway. Prog. Lipid Res. **37**, 317–352(1998).

7. Grechkin, A. N. Hydroperoxide lyase and divinyl ethersynthase. Prostaglandins Other Lipid Mediat. **68–69**, 457–470(2002).

8. Stumpe, M., Feussner, I. Formation of oxylipins by CYP74 enzymes. Phytochem. Rev. 5, 347–357(2006).

9. Farme, E. E., Weber, H. Vollenweider S. Fatty acid signaling in Arabidopsis. Planta. **206**(2):167–174(1998).

10. Brash, A. R., Yu, Z., Boegli, W. E., Schneider, C. The hepoxilin connection in the epidermis. *FEBS J,* **274**(14): 3494-502 (2007).

11. Feussner, I., Wasternack, C., Annu. The lipoxygease pathway Rev. Plant Biol. **53** 275–297(2002).

12. Liavonchanka, A., Feussner, I., Lipoxygenases: Occurrence, functions and catalysis. J. Plant Physiol. **163**, 348–357(2006).

13. Wasternack, C. Jasmonates: An Update on Biosynthesis, Signal Transduction and Action in Plant Stress Response, Growth and Development Ann. Bot. **100**, 681–697(2007).

14. Hsu, P. Y., Tsai, A. L., Kulmacz, R. J., and Wang, L. H. Expression, purification, and spectroscopic characterization of human thromboxane synthase. *J. Biol. Chem.* **274,** 762–769(1999).

15. Balbi, V., Devoto, A. Jasmonate signalling network in *Arabidopsis thaliana*: crucial regulatory nodes and new physiological scenarios New Phytol. **177**, 301–318(2007).

16. Denisov, I. G., Makris, T. M, Sligar S.G. and Schlichting I. Structure and chemistry of cytochrome P450. *Chem. Rev.*, **105**, 2253-2278 (2005).

17. Hughes, R. K., Belfield, E. J., Muthusamay, M., Khan, A., Rowe, A., Harding, S. E., Fairhurst, S. A., Bornemann, S., Ashton, R., Thorneley, R. N. F., Casey, R. Characterisation of Medicago truncatula hydroperoxide lyase (CYP74C3), a water-soluble detergent-free cytochrome P450 monomer whose biological activity is defined by monomer-micelle association. Biochem J **395**, 641–652(2006).

18. Hughes, R. K., Belfield, E. J., Ashton, R., Fairhurst, S. A., Go¨bel, C., Stumpe, M., Feussner, I., Casey, R. Allene oxide synthase from Arabidopsis thaliana(CYP74A1) exhibits dual specificity that is regulated by monomer-micelle association. FEBS Lett **580**:4189–4195(2006).

19. Brash, A. R. Mechanistic aspects of CYP74 allene oxide synthases and related cytochrome P450 enzymes. *Phytochemistry*, **70**, 1522-1531 (2009).

20. Hasemann, C. A., Kurumbail, R. G., Boddupalli, S. S., Peterson, J. A., and Desienhofer j. Structure and function of cytochromes P450:a comparative analysis of three crystal structures Structure **2**, 41-62(1995).

21. Zimmerman, D. C. A new product of linoleic acid oxidation by a flaxseed enzyme. Biochem. Biophys. Res. Commun. **23**, 398–402 (1966).

22. Hamberg, M. Mechanism of corn hydroperoxide isomerase: detection of 12,13(S)-oxido-9(Z),11-octadecadienoic acid. Biochim. Biophys. Acta **920**, 76–84 (1987).

23. Brash, A. R., Baertschi, S. W., Ingram, C. D. & Harris, T. M. Isolation and characterization of natural allene oxides: unstable intermediates in the metabolism of lipid hydroperoxides. Proc. Natl Acad. Sci. USA **85**, 3382–3386 (1988).

24. Song, W. C. & Brash, A. R. Purification of an allene oxide synthase and identification of the enzyme as a cytochrome P-450. Science **253**, 781–784 (1991).

25. Song, W. C., Baertschi, S. W., Boeglin, W. E., Harris, T. M. & Brash, A. R. Formationof epoxyalcohols by a purified allene oxide synthase. Implications for the mechanism of allene oxide synthesis. J. Biol. Chem. **268**, 6293–6298 (1993).

26. Tijet, N. & Brash, A. R. Allene oxide synthases and allene oxides. Prostaglandins Other Lipid Mediat. **68–69**, 423–431 (2002).

27. Matsui, K. Green leaf volatiles: hydroperoxide lyase pathway of oxylipin metabolism. Curr. Opin. Plant Biol. **9**, 274–280 (2006).

28. Vick, B. A. & Zimmerman, D. C. Lipoxygenase and hydroperoxide lyase in germinating watermelon seedlings. Plant Physiol. **57**, 780–788 (1976).

29. Grechkin, A. N. & Hamberg, M. The ‘‘heterolytic hydroperoxide lyase’’ is an isomerase producing a short-lived fatty acid hemiacetal. Biochim. Biophys. Acta **1636**, 47–58 (2004).

30. Itoh, A. & Howe, G. A. Molecular cloning of a divinyl ether synthase. Identificationas a CYP74 cytochrome P-450. J. Biol. Chem. **276**, 3620–3627 (2001).

31. Grechkin, A. N. Hydroperoxide lyase and divinyl ether synthase. Prostaglandins Other Lipid Mediat. **68–69**, 457–470 (2002).

32. Song, W. C. & Brash, A. R. Purification of an allene oxide synthase and identification of the enzyme as a cytochrome P-450. Science **253**, 781–784 (1991).

33. Stumpe, M. & Feussner, I. Formation of oxylipins by CYP74 enzymes. Phytochem. Rev. **5**, 347–357 (2006).

34. Lee, D. S., Nioche, P., Hamberg, M., and Raman, C.S. Structural Insights into the Evolutionary Paths of Oxylipin Biosynthetic Enzymes, *Nature*, vol. **455**, 363–370(2008).

35. Gardner, H. W. Recent investigations into the lipoxygenase pathway of plants. Biochim Biophys Acta. **1084**:221–239(1991).

36. Wasternack, C., Hause, B. Jasmonates and octadecanoids: signals in plant

stress responses and development. Prog Nucleic Acid Res Mol Biol **72**:165–221(2002).

37. Yamaguchi, S., Yokoyama ,M., Iida, T., Okai, M., Tanaka, O., Takimoto, A. Identification of a component that induces flowering of Lemna among the reaction products of a-ketol linolenic acid (FIF) and norepinephrine. Plant Cell Physiol **42**:1201–1209(2001).

38. Suzuk, M., Yamaguchi, S., Iida, T., Hashimoto, I., Teranishi, H., Mizoguch,i M., Yano, F., Todoroki, Y., Watanabe, N., Yokoyam,a M. Endogenous a-ketol linolenic acid levels in short day-induced cotyledons are closely related to flower induction in Pharbitis nil. Plant Cell Physiol **44**:35–43(2003).

39. Hatanaka, A. The fresh green odor emitted by plants. Food Rev Int **12**:303–3509(1996).

40. Noordermeer, M. A., Veldink, G. A., Vliegenthart, J. F. Fatty acid hydroperoxide lyase: a plant cytochrome P450 enzyme involved in wound healing and pest resistance. ChemBioChem **2**:494–504(2001).

41. Arimura, G. I., Kost, C., Boland, W. Herbivoreinduced, indirect plant defences. Biochim Biophys Acta **1734**:91–111(2005).

42. Vancanneyt, G., Sanz, C., Farmaki, T., Paneque M., Ortego, F., Castanera, P.,

Sanchez-Serrano, J. J. Hydroperoxide lyase depletion in transgenic potato plants leads to an increase in aphid performance. Proc Natl Acad Sci USA **98**:8139–8144(2001).

43. Bate, N. J., Rothstein, S. J. C-6-volatiles derived from the lipoxygenase pathway induce a subset of defenserelated genes. Plant J **16**:561–569(1998).

44. Kishimoto, K., Matsu,i K., Ozawa R, Takabayashi, J. Components of C6-aldehyde-induced resistance in Arabidopsis thaliana against a necrotrophic fungal pathogen, Botrytis cinerea. Plant Sci **170**:715–723(2006a)

45. Duan, H., Huang, M. Y., Palacio, K., Schuler, M. A. Variations in CYP74B2 (hydroperoxide lyase) gene expression differentially affect hexenal signaling in the Columbia and Landsberg erecta ecotypes of Arabidopsis. Plant Physiol **139**:1529–1544(2005)

46. Pohnert, G. Diatom/copepod interactions in plankton: the indirect chemical defense of unicellular algae. ChemBioChem **6**:1–14(2005).

47. Grechkin, A. Physiologically active products of plant lipoxygenase pathway. In: KaderJ-C, Mazliak P (eds) Plant lipid metabolism. Kluwer Academic Publishers, Dordrecht, 274–279(1995).

48. Stumpe. M., Kandzia, R., Go¨ bel, C., Rosahl, S., Feussner, I. A pathogen-inducible divinyl ether synthase (CYP74D) from elicitor-treated potato suspension

cells. FEBS Lett **507**:371–376(2001)

49. Weber, H., Chetela,t A., Caldelari, D., Farmer, E. E. Divinyl ether fatty acid synthesis in late blightdiseased potato leaves. Plant Cell 11:485–493 (1999)

50. Schwede T, Kopp J, Guex N, Peitsch MC SWISS-MODEL: an automated protein homology-modeling server. *Nucleic Acids Res* **31**: 3381–33859(2003)

51. DeLano WL *The PyMOL Molecular Graphics System*. California, USA: DeLano Scientific, San Carlos(2002)

요약문

[포도의 *CYP74* family 유전자 cloning 및 재조합 단백질의 발현과 특성 분석]

포도에서 옥시리핀 생합성 관련 유전자를 선발하고 그 기능을 확인하고자 포도의 *CYP74* family 유전자를 선발하였다. 포도에서 분리한 *VvCYP74* 유전자는 open reading frame의 길이가 1452bp 였으며, 483개의 아미노산을 코드하는 것으로 확인되었고, 상동성조사 및 계통분석 등을 통하여 선발한 유전자는 CYP74C subfamily에 속할 가능성이 높은 것을 확인하였다.

이 유전자의 기능을 확인하고자 선발한 유전자를 대장균 발현벡터인 pCWori^{+}에 재구성 한 후 대장균에서 발현하여 재조합단백질을 분리/정제 하였으며, 그 기능을 효소활성분석을 통하여 확인한 결과, oxylipin 생합성에 중요한 역할을 하는 AOS인 것으로 확인되었다.

옥시리핀 생합성 효소인 AOS/HPL의 활성에는 N-terminus 부근의 phenylalanine/leucine 역할이 매우 중요한 것으로 알려져 있어 이 아미노산 잔기의 변화와 활성과의 관련성을 확인하고자 포도에서 선발한 *VvCYP74* 유전자의 100번째 아미노산 잔기 phenylalanine을 leucine으로 치환하였다. 그리고 그 유전자를 대장균에서 발현시켜 재조합단백질 분리/정제한 후 효소활성을 분석하여 본 결과, 기대했던 바와 같이 HPL 활성을 나타내는 것을 확인할 수 있었고, 이와 더불어 EAS 활성도 나타내는 것을 확인하였다. 이러한 결과로 볼 때 옥시리핀 생합성효소인 AOS와 HPL의 활성에는 N-terminus 부근의

phenylalanine/leucine의 역할이 매우 중요하다는 것을 확인하였다.

결론적으로, 본 연구를 통하여 포도에서 옥시리핀 생합성 관련 유전자(VvCYP74C)를 선발하였고, 그 기능을 확인한 결과 AOS 활성이 있는 것으로 확인되었다. 이 유전자의 100번째 아미노산 잔기 phenylalanine을 leucine으로 치환하여 기능을 분석하여 본 결과, 기능이 AOS에서 HPL로 변화하는 것을 확인하였으며, 이와 더불어 EAS활성도 보이는 것을 확인하였다. 이러한 결과는 향후 포도의 병해충저항성을 증진하는 분자생물학적 연구에 있어 매우 중요한 기반이 될 것으로 사료된다.

ACKNOWLEDGEMENT

너희는 먼저 그의 나라와 그의 의를 구하라 그리하면 이 모든 것을 너희에게 더 하시리라. 그러므로 내일 일을 위하여 염려하지 말라. 내일 일은 내일 염려할 것이요 한날 괴로움은 그날에 족하니라. (마태복음 6장 33-34)